2

The dynamics of slider bearings during contacts between slider and disk

by Richard C. Benson Chisin Chiang Frank E. Talke

The dynamics of a "mini-Winchester" magnetic recording slider are studied during contacts with a hard, rotating memory disk using numerical simulation. An on-line solution of the Reynolds equation is used to calculate the air-film pressure, and a "coefficient-of-restitution" model is used to describe intermittent slider/disk contacts. Studies are made to identify system configurations which reduce the possibility of a "head crash" during contact start/stop.

Introduction

This paper is concerned with an important problem in magnetic storage technology: namely, intermittent contacts between a magnetic recording slider and a hard disk. We are interested in the dynamics of a hydrodynamically supported magnetic recording slider flying over a hard, rotating disk and making occasional contacts with the disk. Under steady-state conditions the slider is flying over the disk at a nominal spacing of $0.3 \mu m$ [1]. The air bearing that supports the

©Copyright 1989 by International Business Machines Corporation. Copying in printed form for private use is permitted without payment of royalty provided that (1) each reproduction is done without alteration and (2) the *Journal* reference and IBM copyright notice are included on the first page. The title and abstract, but no other portions, of this paper may be copied or distributed royalty free without further permission by computer-based and other information-service systems. Permission to *republish* any other portion of this paper must be obtained from the Editor.

slider is designed to prevent contacts between the slider and the disk. However, contacts between the slider and the disk are inevitable during start/stop of the disk file, when the airbearing pressure is insufficient to support the slider completely. Contacts can also occur during track accessing or due to mechanical disturbances of the slider/disk interface. Under adverse conditions these contacts may terminate in a "head crash," i.e., a catastrophic failure of the recording system.

In References [2–4] experimental data are reported that describe head/disk collisions in detail. These studies show that, as a disk accelerates, the slider passes through the stages of (1) steady rubbing against the disk, (2) intermittent slider/disk contact, and (3) "flying" without contact. Mathematical models for the three stages follow from very different lubrication theories. At low disk speeds, boundary lubrication prevails and Coulomb-type friction models are appropriate. At high disk speeds, the solid surfaces are separated by a thin air film, and the physical situation is governed by the Reynolds equation of lubrication [5, 6].

Investigations of the transition region (2) are far fewer in number and much more recent. Kita et al. [3] and Kawakubo et al. [4] have studied the quasi-static takeoff of a slider. Their interest, in part, was to determine the solid-body contact forces that contribute to friction and wear. Ponnaganti et al. [7, 8] have modeled the slider dynamics (with the disk at full speed) when a single large asperity passes along one of the slider rails. They found that head/disk contacts can result in "head crashes" when the front edge of the slider strikes the disk. In other

circumstances a front-edge collision is avoided, and the slider resumes normal flying once the asperity passes from beneath the rail.

Dynamic simulations of the transition from sliding to flying have been conducted by Benson and Talke [9, 10] for slow disk speeds associated with start/stop operation of a disk file. In these investigations, as well as in [7, 8], a "coefficient-of-restitution" model was used to simulate the vertical and horizontal loads that occur during impact. In [9] it was found that an initial disturbance of the slider leads to a chain reaction of collisions, which occur in clusters at the corners. In [10] it was observed that certain collision patterns have increasing amounts of energy being transferred from the disk to the slider, thereby increasing the impulse amplitude between slider and disk for subsequent impacts. This behavior was labeled unstable, and a "window of vulnerability" was identified for those conditions.

The dynamic simulations of [7–10] are limited in their treatment of the Reynolds equation. In [7] and [8] a simplified version of the Reynolds equation, appropriate for very high bearing numbers, was used. In [9] and [10] the Reynolds equation was solved for various steady-state flying heights which permitted the replacement of the Reynolds equation by a table interpolation procedure. One resorts to such approximations because an on-line, numerical solution of the Reynolds equation is very time-consuming and slows the process of acquiring data on the total system response.

With the basic information of [7–10] known to us, we wish to make a more detailed study of the slider instability that was identified in [10]. In particular, we wish to trace the slider through periods of collisions, and to more accurately compute the threshold of instability as a function of friction and perturbing velocity. For these reasons, and in the interest of achieving better agreement between experimental and theoretical results, it is apparent that the simulation of the head/disk dynamics should include an on-line solution of the Reynolds equation. We accomplish that task by coupling the numerical solution of the Reynolds equation from Grove et al. [6] with the equations of motion of the slider [9, 10].

We discovered that the event of a head crash is subjectively defined. A slider that collides repeatedly and violently with the disk may, after sufficient time, resume steady flying. Thus, even though a stable flying behavior is ultimately achieved, the latter situation cannot be considered acceptable from the point of view of materials interaction and wear.

In this paper, we analyze the dynamic behavior of the slider as a function of both the coefficient of friction and the coefficient of restitution. We study the time sequence of slider contacts for a typical "mini-Winchester" recording slider, and we determine the regions of stable and unstable flying behavior for various values of the coefficient of friction and the "coefficient of restitution." In addition, we

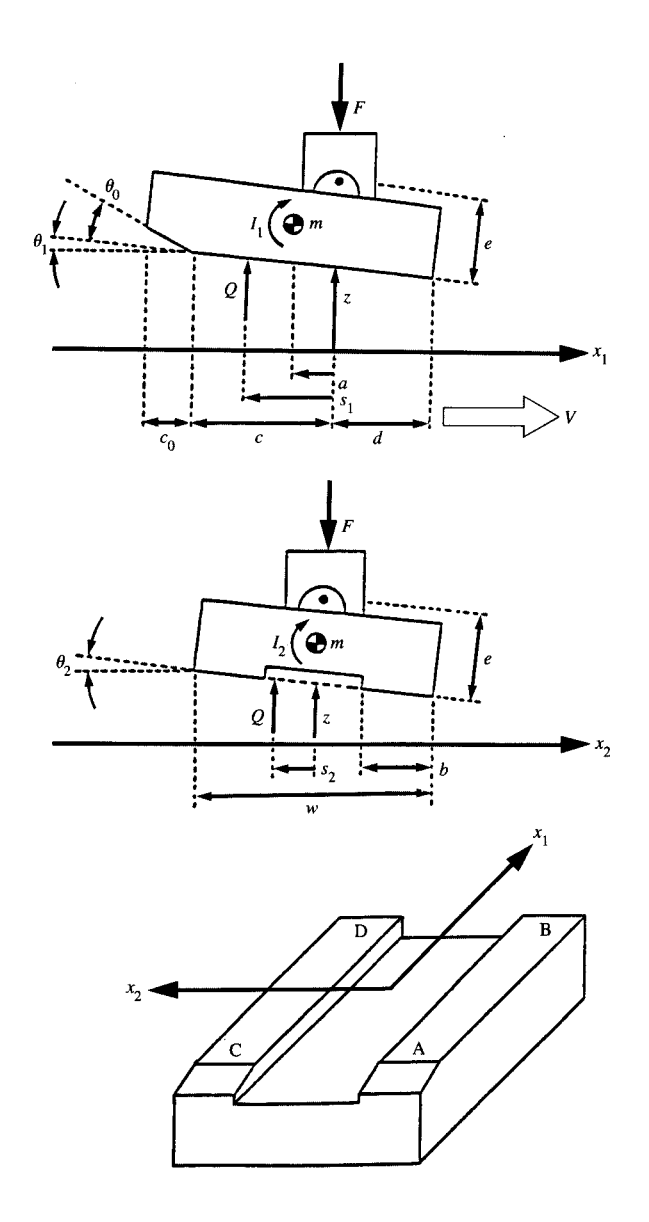


Figure 1
Schematic of head/disk interface.

investigate the dependence of slider dynamics on the initial conditions and identify contact situations which reduce the possibility of a head crash.

Mathematical model

• Geometry

The mechanical system considered in this investigation is shown schematically in Figure 1. The slider is attached to a

Model for asperities

cantilever suspension by a small leaf spring which permits two rotations, pitch θ_1 and roll θ_2 . The suspension spring is flexible in the vertical direction, thus adding a third degree of freedom to the slider in the z-direction. The z-variable is measured along a line through the gimbal and perpendicular to the plane of the disk. To locate points under the "footprint" of the slider, coordinates x_1 and x_2 are used. The origin, $x_1 = x_2 = 0$, lies directly beneath the gimbal. One of the four corners of the slider (marked A, B, C, and D) corresponds to the minimum spacing between the slider and the disk.

For the problems under investigation, the spacing between the slider and the disk is so small that roughness of the disk surface must be considered. We use a simple model proposed originally by Kita et al. [3], in which we assume that the Reynolds equation is valid as long as the minimum spacing between slider and disk is larger than the disk roughness. Whenever the minimum spacing is equal to the disk roughness, a contact between slider and disk is assumed to occur and the solution of the Reynolds equation is continued with new initial conditions. The surface of the disk is taken to be a plane with protruding asperities (Figure 2). All vertical measurements are made from the "base plane," i.e., the plane at the base of the asperities. Compared to the air-film spacing, the asperities are sufficiently scattered that they do not interfere with the fluid flow. Compared to the slider-rail dimensions, however, the asperities are sufficiently numerous that solid-body contact always occurs

at the tops of the asperities. Furthermore, we assume that the asperities are all approximately of the same height, h_0 .

As seen from Figure 1, the disk moves with velocity V. At steady state the slider is oriented so that the resultant force, Q, from the air-bearing pressure is equal, opposite, and colinear $(s_1 = s_2 = 0)$ to the preload, F, acting through the gimbal. During start/stop and dynamic excursions, however, the slider is not in steady state, and inertial loads due to slider acceleration have to be considered. The mass of the slider is m, and its center is located at $x_1 = -a$, $x_2 = 0$. The mass moments of inertia for pitching and rolling motions are I_1 and I_2 , respectively. A final source of loading arises from the solid-body contacts between the slider and disk. At the instant of collision, impulsive loads act at the contact point, causing sudden changes in the vertical, pitch, and roll motions of the slider.

• Slider dynamics

When not in contact with the disk, the slider flies according to the following differential equations for vertical displacement, pitch, and roll:

$$m\ddot{z} + ma\ddot{\theta}_1 = Q - F,\tag{1}$$

$$ma\ddot{z} + I_1\ddot{\theta}_1 = S_1Q - T_1, \qquad (2)$$

$$I_2\ddot{\theta}_2 = S_2Q - T_2. \tag{3}$$

In Equations (1)–(3), the left-hand-side terms denote inertial loads, and dots represent time derivatives. On the right-hand side are the external loads from the air pressure and the suspension preload. Air-pressure results are found from the following integrals over the surface area A of the slider rails:

$$Q = \int_{A} [p(x_1, x_2, t) - p_0] dA, \tag{4}$$

$$S_1 Q = \int_A x_1 [p(x_1, x_2, t) - p_0] dA,$$
 (5)

$$S_2 Q = \int_A x_2 [p(x_1, x_2, t) - p_0] dA.$$
 (6)

In the above equations $p(x_1, x_2, t)$ is the air-film pressure, which varies with location and time. The air-film pressure is governed by the Reynolds equation [11]

$$\frac{\partial}{\partial x_1} \left[h^3 p \frac{\partial p}{\partial x_1} + 6\lambda p_0 h^2 \frac{\partial p}{\partial x_1} \right] + \frac{\partial}{\partial x_2} \left[h^3 p \frac{\partial p}{\partial x_2} + 6\lambda p_0 h^2 \frac{\partial p}{\partial x_2} \right]$$

$$=6\eta V \frac{\partial}{\partial x}(hp) + 12\eta \frac{\partial}{\partial t}(hp), \tag{7}$$

subject to the boundary condition

$$p = p_0, (8)$$

where p_0 denotes the ambient pressure at the edges of the

slider rails. Parameters in Equation (7) which have not been previously identified are the air viscosity η and the mean free path of air molecules λ . Terms involving λ are "slip-flow" corrections accounting for rarefaction effects at very small spacings [11].

• Contact

The spacing h is a function of location x_1 and x_2 and the three variables which set the rigid-body orientation of the slider—z, θ_1 , and θ_2 :

$$h(x_1, x_2, t) = \mathcal{I}[x_1, x_2, z(t), \theta_1(t), \theta_2(t)]. \tag{9}$$

The slider geometry determines the form of the function \mathfrak{I} . For a typical mini-Winchester recording head with a taper/flat bearing geometry (Figure 1), the spacing is given by

$$h = z - x_1 \theta_1 - x_2 \theta_2$$
 when $-c \le x_1 \le d$

and
$$\frac{w}{2} - b \le |x_2| \le \frac{w}{2}$$
,

and

$$h = z - x_1 \theta_1 - x_2 \theta_2 - (x_1 + c)\theta_0$$
when $-(c + c_0) \le x_1 \le -c$
and $\frac{w}{2} - b \le |x_2| \le \frac{w}{2}$. (10)

This expression can be differentiated to give the velocity by which points on the slider approach the disk,

$$U = -\dot{z} + x_1 \dot{\theta}_1 + x_2 \dot{\theta}_2. \tag{11}$$

Impacts are assumed to occur when the spacing at any point of the slider equals the height of the asperities, i.e.,

$$h(x_1, x_2) = h_0. (12)$$

In this case, the equations of motion of the slider must be modified to read

$$m\ddot{z} + ma\ddot{\theta}_1 = Q - F + q\delta(t - t^*), \tag{13}$$

$$ma\ddot{z} + I_1\ddot{\theta}_1 = S_1Q - T_1 - (x_1 + e\mu)q\delta(t - t^*),$$
 (14)

$$I_{2}\ddot{\theta}_{2} = S_{2}Q - T_{2} - x_{2}q\delta(t - t^{*}), \tag{15}$$

where $\delta(t-t^*)$ is the delta function, t^* denotes the time when a contact occurs, $q\delta(t-t^*)$ is the impulsive force during contact, and $-(x_1+e\mu)q\delta(t-t^*)$ and $-x_2q\delta(t-t^*)$ are the impulsive moments in the pitch and roll directions, respectively, associated with the contact. By the uniform roughness assumption made earlier, contacts will occur at one of the four corners of the rail "flats":

A: front, left:
$$x = -c$$
, $x = -w/2$, (16)

B: back, left:
$$x = d$$
, $x = -w/2$, (17)

C: front, right:
$$x = -c$$
, $x = w/2$, (18)

D: back, right:
$$x = d$$
, $x = w/2$. (19)

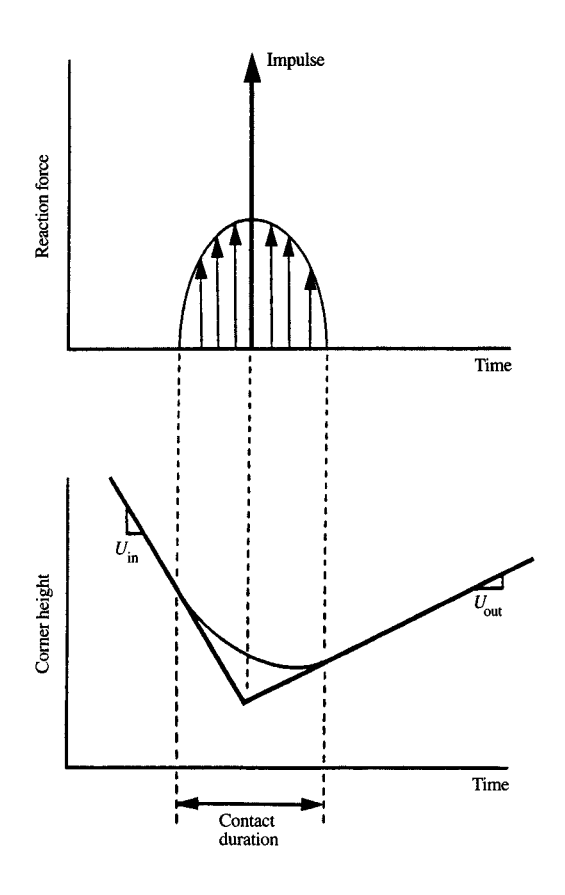


Figure 3

Model for impact.

When impact occurs, a complicated mechanical process takes place: Some of the kinetic energy of the slider is stored in elastic strain energy of the two bodies and then returned to the slider. Some energy is propagated away in waves. Some is lost in plastic deformation, especially if highly concentrated forces occur on asperity peaks. Due to geometrical effects, the slider may even gain energy from the impact.

Because the numerical calculation of the details of the impact process, based on first principles, would be exceedingly difficult and time-consuming, a computationally less demanding coefficient-of-restitution model was used. A schematic illustration of this model is shown in Figure 3 for the simple case of a slider contacting a stationary disk. In Figure 3, the dashed lines represent the vertical position and contact force experienced by a corner of the slider as it contacts the disk. There is a finite, albeit small, time duration of contact. Due to energy losses during the collision, the rebound velocity of the slider, $U_{\rm out}$, is less than

a = 0.028	mm
b = 0.686	mm
c = 1.788	mm
d = 0.382	mm
e = 1.000	mm
F = 0.0932	N
h = 0.050	μm
$I_1 = 0.143$	$nN \cdot s^2 \cdot m$
$I_2 = 0.074$	$nN \cdot s^2 \cdot m$
m = 0.071	g
p = 101.0	kN/m^2
V = 2.000	m/s
w = 3.200	mm
$\lambda = 0.06$	μ m
$\eta = 18.1$	μ N·s/m ²
$\theta_0 = 0.0145$ rad	

the downward velocity before impact, U_{in} . In our model, we assume that the ratio of outgoing and incoming velocities is a constant for a given slider/disk materials combination, i.e.,

$$\alpha = \frac{U_{\text{out}}}{U_{\text{in}}}.$$
 (20)

The coefficient of restitution, α , is related to the time integral of the contact load (i.e., the impulse) and the mass of the slider. Knowledge of the impulse allows us to compute the coefficient of restitution, and vice versa. Here, we assume that α is the known quantity, and we replace the loading curve of Figure 3 with the resultant impulse. Consequently, the rounded corner in the graph of the position of the slider is replaced with the sharp corner of an instantaneous velocity jump.

To estimate the duration of contact, one could set the condition that the corner spacing be within a specified multiple of the nominal roughness (say $1.5h_0$ or $2.0h_0$). This scheme is motivated by Figure 3, which shows the sharpened corner of the instantaneous-velocity jump curve penetrating more deeply than the rounded corner of the finite-duration contact curve. It is likely that more than one corner will be deemed to be simultaneously in contact (particularly the rear-corner pair, B and D). The total blending of contacts would then define the extended duration of contact for the slider with three degrees of freedom of rigid-body motion. (Ponnaganti et al. [7, 8] use all six.) The extended contact would correspond roughly to the duration of corner "cluster" impacts described in [9].

Disk velocity complicates the impact process in two ways. First, due to the relative motion between slider and disk, a frictional impulse must be taken into account in addition to vertical impulse. For Coulomb friction assumed in our model, we note that the tangential impulse is related to the vertical impact through the coefficient of friction.

A second effect arising from disk velocity is a "wedging" action as the asperities strike against the inclined surface of the slider; i.e., a slider need not be moving toward the disk to receive an impulse from the disk. Especially large impulses occur if asperities hit the slider in the inclined taper section of the slider.

Following [9], the component velocity jumps that occur when the slider strikes the disk are

$$\Delta \dot{z} = Jq, \tag{21}$$

$$\Delta \dot{\theta}_1 = J_1 q, \tag{22}$$

$$\Delta \dot{\theta}_2 = J_2 q,\tag{23}$$

and the impulse of the collision is

$$q = \frac{(1+\alpha)(U+\epsilon V)}{J - x_1 J_1 - x_2 J_2}. (24)$$

In Equation (21), the J coefficients are defined by the inertia and mass of the slider,

$$J = \frac{I_1 + ma(x_1 + e\mu)}{mI_1 - (ma)^2},$$
(25)

(20)
$$J_1 = -\frac{ma + m(x_1 + e\mu)}{mI_1 - (ma)^2},$$
 (26)

$$J_2 = \frac{X_2}{I_2},\tag{27}$$

and ϵ is the slope of the slider at the point of impact,

$$\epsilon = \theta_1$$
 at rear corners B and D, (28)

$$\epsilon = \theta_1 + \theta_0$$
 at front corners A and C. (29)

Note that we assume that collisions at the front corners take place on the taper side of the taper/flat juncture.

Numerical solution

For numerical solution of the Reynolds equation we used the two-dimensional, dynamic finite-difference program of Grove et al. [6]. We typically used 201 nodes along each rail length, and 21 nodes across each rail width. The crosswise nodes were equally spaced. The lengthwise nodes were unevenly spaced to give greater resolution in the highpressure-gradient regions near the taper/flat juncture and the trailing edge. A typical time step during slider flying was 0.1 μs. Shorter intervals were used to bracket collisions.

The benefits and penalties of the on-line solution were as expected. Compared to the "table method" used in [9, 10], our method provided a much better estimation of the

bearing stiffness and damping characteristics. Because these are velocity- and excursion-dependent quantities, we would have required a very large table to represent the bearing loads through some of the extreme motions of an unstable slider. The stiffness values used in [9, 10] are based on quasistatic, moderate excursion conditions, and are too low for use here. The penalty for the increased accuracy is decreased convergence speed. A simulation that took several minutes on an IBM PC by the table method now requires several hours on an Aliant or Sun workstation.

Computation of the slider rigid-body motion was done by a simple predictor-corrector integration of Equations (1)–(3).

Results

• Threshold of instability

In Figures 4–23, numerical results are shown for the motion of a slider using the slider/disk parameters given in **Table 1** and a disk velocity of 2 m/s. Due to the low velocity, the slider flies very close to the disk, with steady-state values of

$$z = 0.115 \ \mu \text{m},$$
 (30)

$$\theta_1 = 13.5 \ \mu \text{rad},\tag{31}$$

$$\theta_2 = 0.0 \ \mu \text{rad.} \tag{32}$$

The asperity height above the base plane was taken to be

$$h_0 = 0.050 \ \mu \text{m}.$$
 (33)

The first set of data to be considered appears in Figures 4–8. Here, the steady flying state of the slider was disturbed by giving it the following initial velocities:

$$\dot{z} = -0.01 \text{ m/s},$$
 (34)

$$\dot{\theta}_1 = 5.0 \text{ rad/s}, \tag{35}$$

$$\dot{\theta}_2 = 10.0 \text{ rad/s.} \tag{36}$$

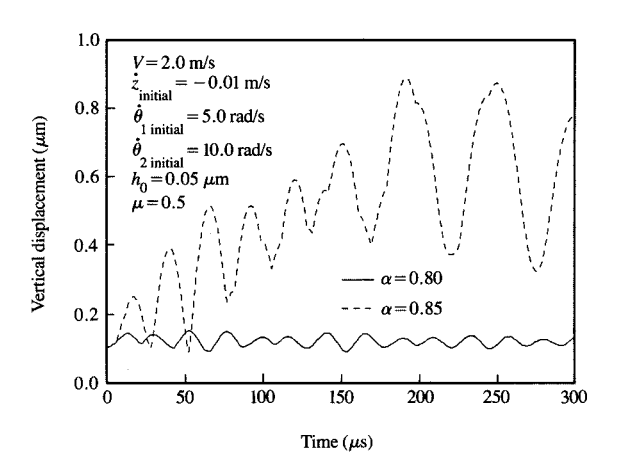
The coefficient of friction was set at

$$\mu = 0.50,$$
 (37)

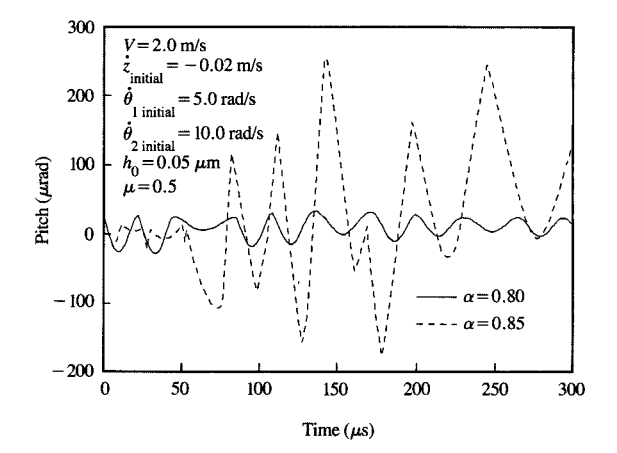
and two values of the coefficient of restitution were considered, namely

$$\alpha = 0.80$$
 and $\alpha = 0.85$. (38)

Despite the closeness of the two values of the coefficient of restitution, the dynamic response of the slider is completely different. At the lower coefficient of restitution, the slider oscillates near its steady-state values, as shown by the solid lines in **Figures 4**, **5**, and **6**. Furthermore, as can be seen from the impact history of the slider shown in **Figure 7**, the slider strikes the disk only eight times, always at the rear corners. (Note that the letter above the spike denotes the corner of impact.) We observe that the largest impulse is $0.73 \mu \cdot Ns$, occurring immediately after the initial disturbance, and that all successive impacts are smaller in magnitude than the initial impact.



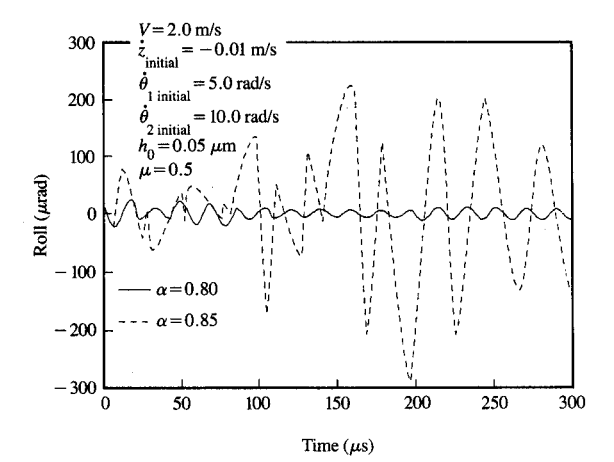
Vertical displacement of slider vs. time for $\alpha = 0.80$ and $\alpha = 0.85$.



Pitch of slider vs. time for $\alpha = 0.80$ and $\alpha = 0.85$

By contrast, the slider with $\alpha = 0.85$ shows erratic motion for all three modes of motion, as shown by the dotted line in Figures 4, 5, and 6. In addition, the impact history of the slider (Figure 8) indicates that the magnitude of successive impacts increases substantially above that of the initial contact. Twenty-two impacts with magnitude greater than the initial impact are observed in the first 300 μ s of simulation (Figure 8). Furthermore, contacts occur at all





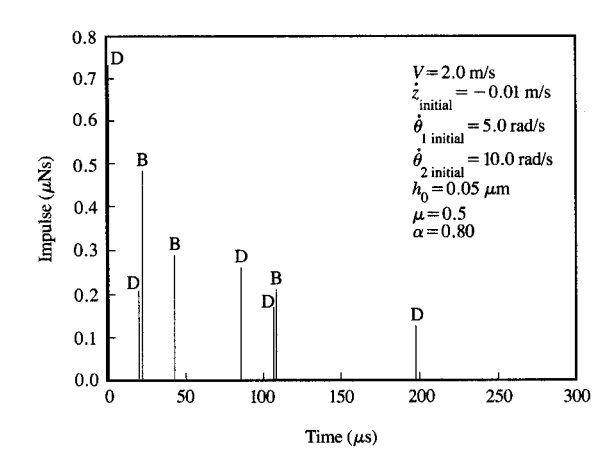


Figure 6 Roll of slider vs. time for $\alpha = 0.80$ and $\alpha = 0.85$.

Figure 7

Slider/disk impact history for $\alpha = 0.80$.

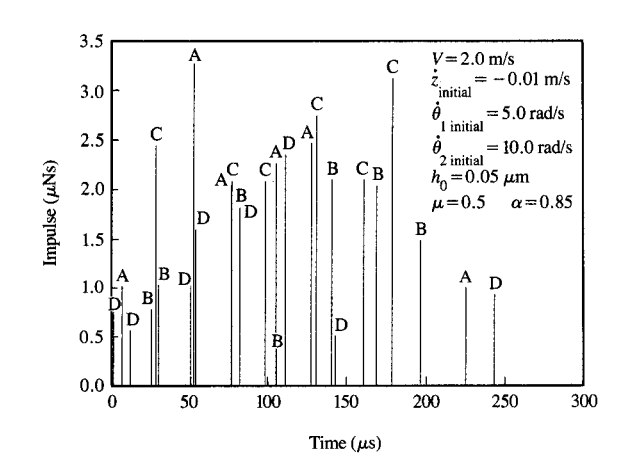


Figure 8 Slider/disk impact history for α =0.85.

four corners. Holding all other parameters constant, we found that $0.80 < \alpha < 0.85$ brackets the only separating point of the two types of behavior. For values of the coefficient of restitution less than 0.80, successive contacts decrease in magnitude, while for values of the coefficient of restitution above 0.85, there are contacts that are larger than the initial contact.

Even the most erratic slider motions may eventually settle back to steady state. This is shown in **Figures 9–11**, which are extensions of the $\alpha=0.85$ trajectories of Figures 4–6 for long time periods. Here we note that the slider returns to steady state after 1500 μ s of simulation. Clearly, standard tests of stability are not applicable in determining whether a contact sequence is stable or unstable. However, since contact sequences with increasing amplitude are likely to cause more damage to the slider/disk interface than sequences with decreasing amplitudes, we have arbitrarily termed sequences with increasing amplitudes unstable, and those with decreasing amplitudes stable.

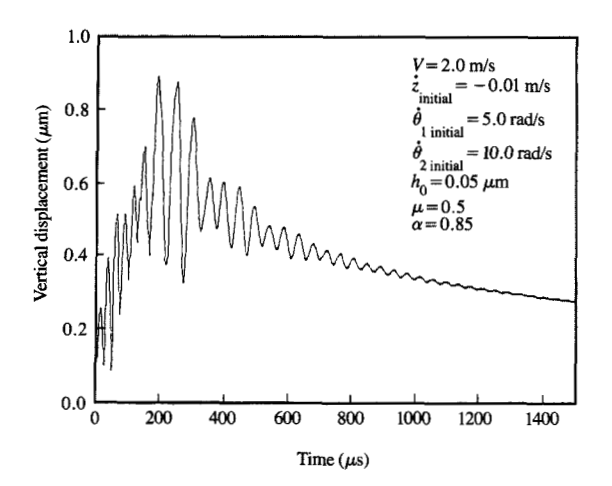
• Influence of friction

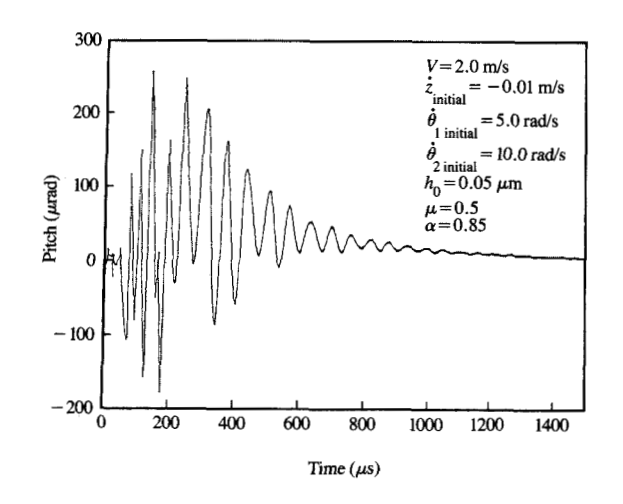
The behavior of the slider during impacts is also affected by the coefficient of friction. This is shown in **Figures 12–16**, which are the analogs of Figures 4–8, but with the coefficient of friction raised to

$$\mu = 1.0. \tag{39}$$

We observe that the threshold between stable and unstable contact dynamics is now reduced to a coefficient of restitution value between $\alpha = 0.65$ and 0.70. Thus, increased friction tends to reduce the critical value of α , since the frictional drag acts to pitch the slider down toward a front-corner impact.

In Figure 17 the demarcation between stable and unstable contact behavior is shown in the friction-restitution plane. We observe that the region of stable contact behavior decreases almost linearly with increasing μ ; i.e., large μ values correspond to low values of α , while small μ values



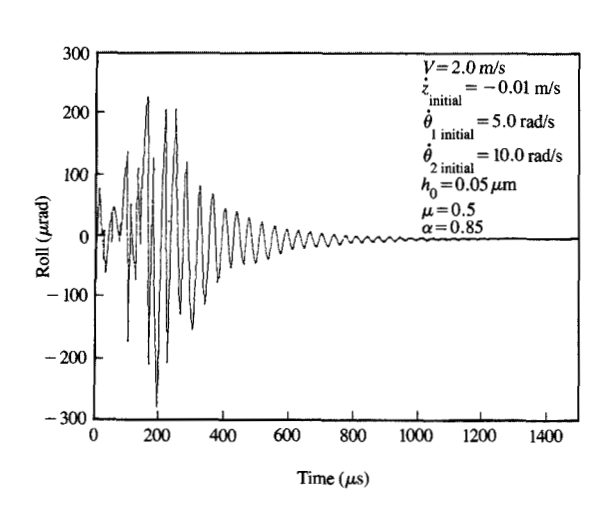


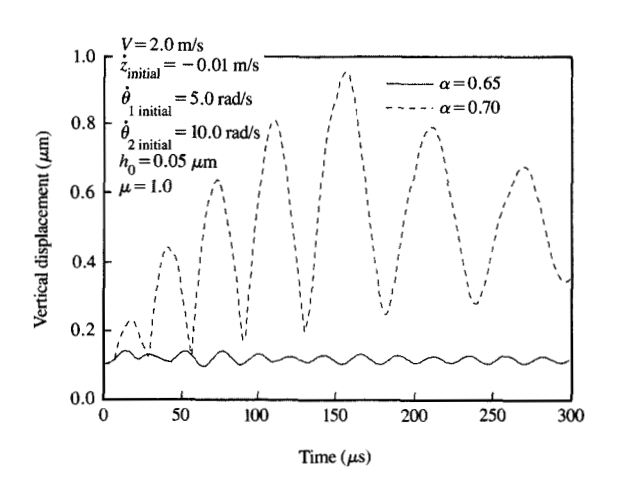
eranta G

Long-time behavior of vertical displacement of slider for $\alpha = 0.85$.

Figure 10

Long-time pitch behavior of slider for $\alpha = 0.85$.





Emilia II

Long-time roll behavior of slider for $\alpha = 0.85$.

slider after a large initial disturbance. The coefficient of

correspond to high α values. The results of Figure 17 should be considered only as a trend, since the demarcation between stable and unstable contact behavior is also a function of slider geometry, the surface roughness of the disk, and the magnitude of the initial perturbation.

 $\mu = 0.5,\tag{40}$

Vertical displacement of slider vs. time for high friction coefficient

and the initial vertical approach velocity between slider and disk is doubled to

 $\dot{z} = -0.02 \text{ m/s}.$ (41)

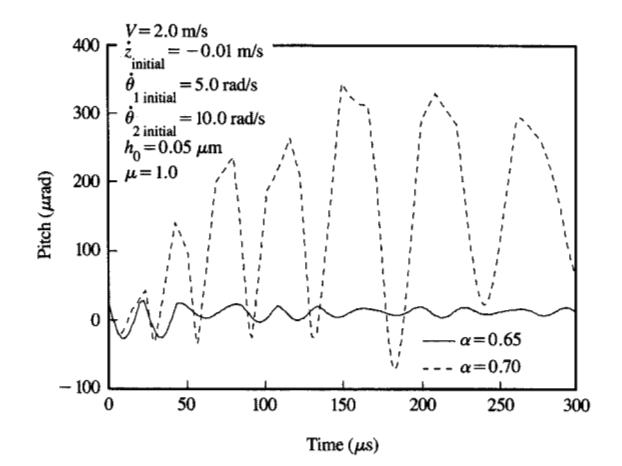
Three coefficients of restitution are considered:

 $(\mu = 1.0, \alpha = 0.65, \alpha = 0.70)$

friction is reset to

• Dependence on the initial disturbance

To illustrate this last point, we present the data of Figures 18-23 for the flying behavior and contact histories of the



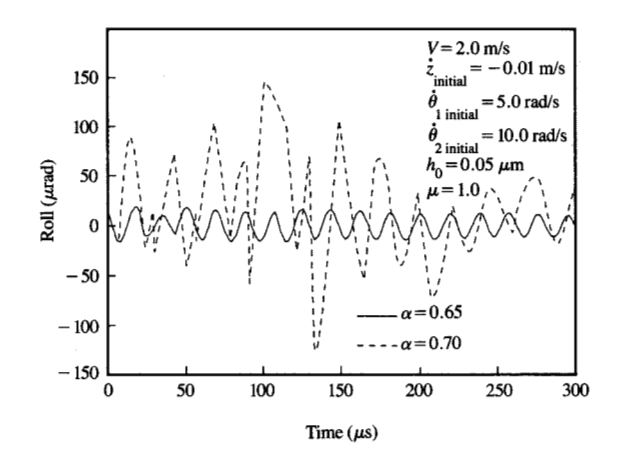
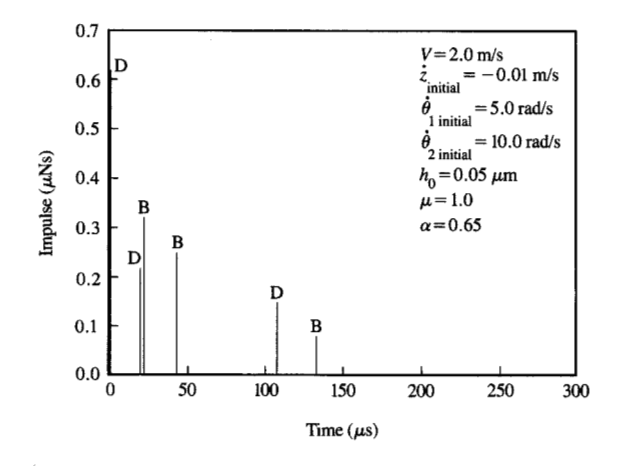


Figure 18

Pitch of slider vs. time for high friction coefficient ($\mu = 1.0$, $\alpha = 0.65$, $\alpha = 0.70$).

Figure 14

Roll of slider vs. time for high friction coefficient ($\mu = 1.0$, $\alpha = 0.65$, $\alpha = 0.70$).



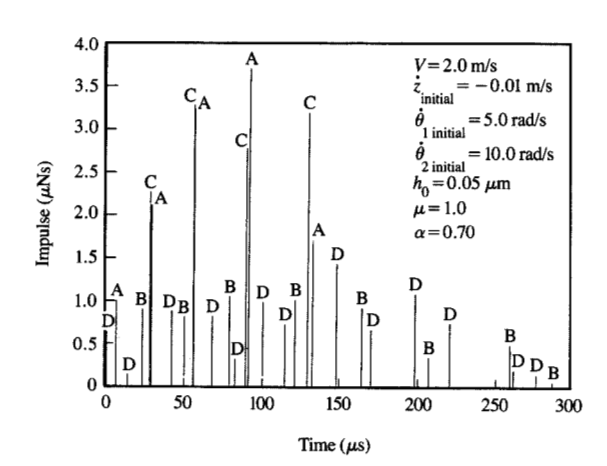


Figure 15

Slider/disk impact history for high friction coefficient ($\mu = 1.0$, $\alpha = 0.65$).

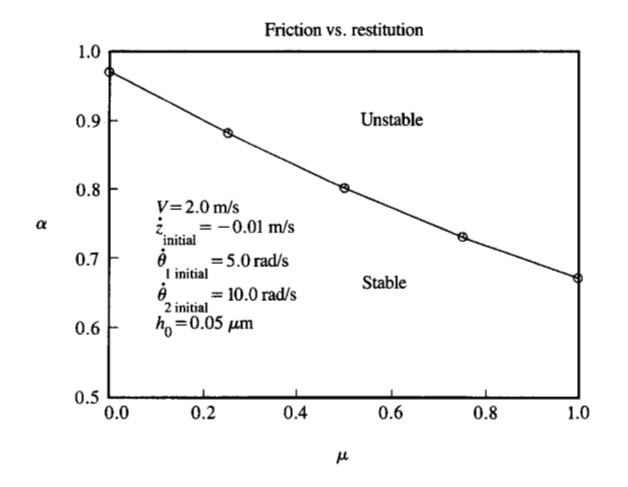
Hall Garage

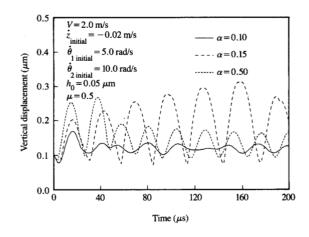
Slider/disk impact history for high friction coefficient ($\mu = 1.0$, $\alpha = 0.70$).

$$\alpha = 0.50, \quad \alpha = 0.15, \quad \text{and} \quad \alpha = 0.10.$$
 (42)

Graphs for vertical motion, pitch, and roll are presented in Figures 18–20, and impact histories for the three coefficients of restitution are shown in Figures 21–23. We observe from Figures 18–20 that the slider behavior for the lowest coefficient of restitution value corresponds to low-amplitude

oscillatory motion around the steady-state flying behavior, i.e., a behavior similar to that of the $\alpha=0.80$ case in Figures 5-7 for small initial disturbance. However, the results for $\alpha=0.15$ and $\alpha=0.50$ show large excursion from equilibrium, with substantial discontinuities in displacement, pitch, and roll velocities. From the impact histories shown in Figures 18-20, we note that the $\alpha=0.10$ case can be

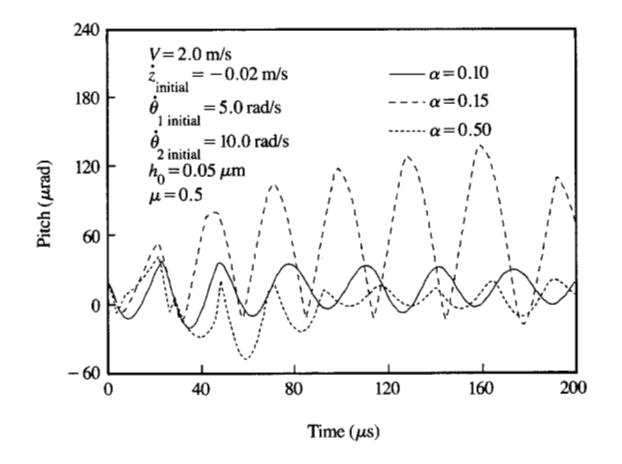


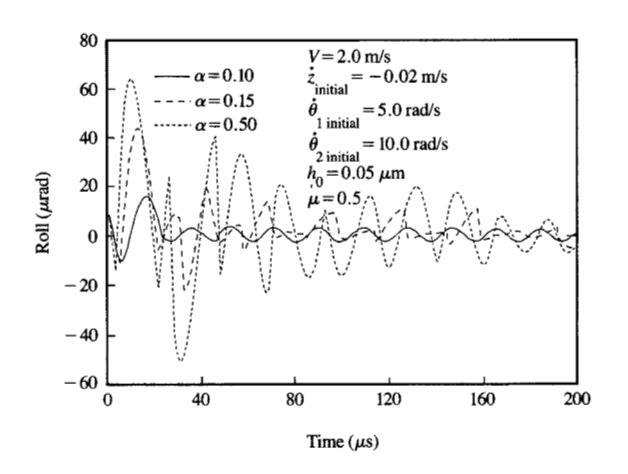


Regions of stable and unstable impact as a function of μ and α .

Figure 18

Vertical displacement of slider vs. time for large initial disturbance $(\alpha = 0.50, \alpha = 0.15, \alpha = 0.10)$.





Pitch of slider vs. time for large initial disturbance ($\alpha = 0.50$, $\alpha = 0.15$, $\alpha = 0.10$).

Figure 21

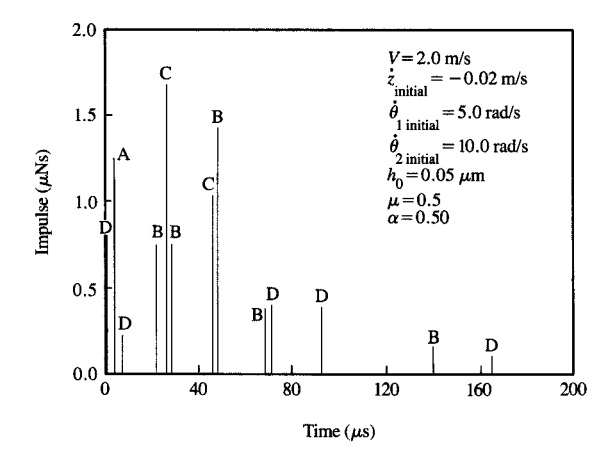
Roll of slider vs. time for large initial disturbance ($\alpha = 0.50$, $\alpha = 0.15$, $\alpha = 0.10$).

described as stable, while the $\alpha=0.15$ and $\alpha=0.50$ cases are unstable. Thus, increasing the initial approach velocity reduces the critical value of the coefficient of restitution that divides stable and unstable slider contact behavior.

Discussion

The results of our numerical simulation can be used to analyze the possibility of head crashes in disk files for various material combinations. To do this, we recall that the region of instability increases as the coefficient of friction increases. From start/stop and constant-speed friction tests, it is well known that the coefficient of friction increases with the number of start/stop cycles. This increase is found to be especially pronounced in thin-film metallic disks coated with a protective carbon overcoat. Here, typical values of the coefficient of friction are of the order of 0.25 to 0.3 for a new







Slider/disk impact history for large initial disturbance ($\alpha = 0.50$).

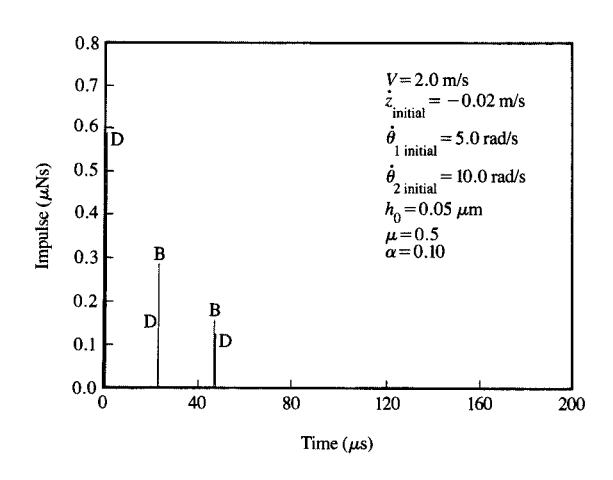


Figure 23

Slider/disk impact history for large initial disturbance ($\alpha = 0.10$).

disk, while values of the order of 0.6 to 1.0 are common after extended wear testing. Thus, for those disks, the region of slider instability increases with time due to the increased friction coefficient, and the tendency of the slider toward instability increases.

From the numerical results we have observed that the transition from stability to instability is quite abrupt. At the threshold value of the coefficient of restitution, the slider barely hits or misses a front corner. Front-corner collisions

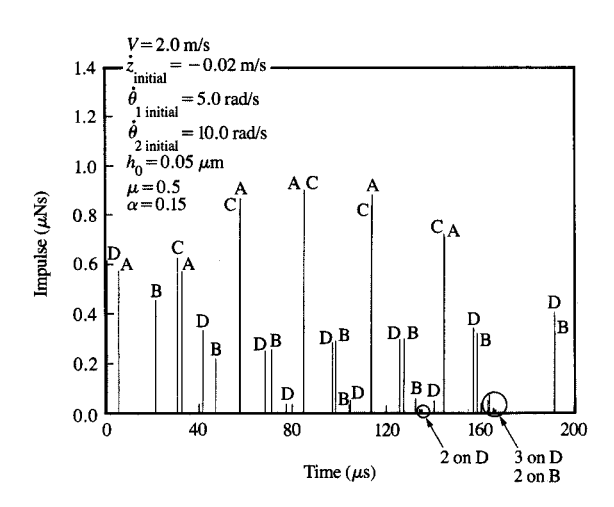


Figure 22

Slider/disk impact history for large initial disturbance ($\alpha = 0.15$).

generally cause violent slider dynamics, as may be seen, for instance, by comparing Figures 7 and 8. Although it is impossible to say whether a front-corner contact will always lead to a head crash, it seems justifiable to assume that avoidance of front-corner contacts improves the tribological behavior of the head/disk interface. We have also found it important to reduce the value of the coefficient of friction as well as the coefficient of restitution in order to achieve as large a window of stable contact behavior as possible.

To obtain a first-order approximation for the numerical value of the coefficient of restitution, we have measured the rebound of a small sphere that is being dropped on the disk, resulting in a calculated value for the coefficient of restitution of the order of $\alpha=0.5$. Additional experiments have indicated that the coefficient of restitution is influenced by the impulse velocity as well as by the size of the contact region. Thus, future simulations may need to include the dependence of the coefficient of restitution on impact velocity and asperity contact size.

The dependence of the contact behavior on the coefficient of restitution suggests that one should try to select slider/disk combinations that reduce the coefficient of restitution, thereby increasing the stability of slider bearings during transition. It is questionable, however, whether much progress can be made in this direction, since very little freedom is available in the selection of appropriate slider/disk materials.

It is interesting to note that increases in the coefficient of restitution in the unstable region do not necessarily produce increasingly worse impact histories in terms of the *number* of slider/disk contacts. This is shown clearly by comparing the impact histories in Figures 21 and 22, where we note a large

number of contacts for the $\alpha=0.15$ case and fewer contacts in the $\alpha=0.50$ case. The $\alpha=0.50$ slider in Figure 21 avoids repeated front-corner impacts primarily due to the coincidence that the vertical displacement reaches maximum values when the pitch goes negative at t=40, 60, and 80 μ s. However, the $\alpha=0.50$ case should not be considered stable, since there are four impacts with greater magnitude than the initial impact.

A further observation to be made from the above case is related to roll motion. The $\alpha=0.50$ slider has more of its kinetic energy in side-to-side roll motion than the slider in the $\alpha=0.15$ case. This suggests an interesting design challenge. Since occasional contacts with asperities are inevitable, it is apparent that the slider needs some degree of flexibility to move out of the way of asperities. On the basis of the above results, it would seem preferable for that to be accomplished through roll, while maintaining or increasing positive pitch. Impacts would not be eliminated or reduced in number, but they could be kept near the safe rear corners. There may be slider designs that lead to hydrodynamically stiff bearings in the vertical motion and the pitch, yet have a "sacrificial" flexibility in the roll motion.

The observation that increased pitch angles improve the dynamic performance of slider bearings by avoiding frontcorner contacts is in agreement with data presented by Gatzen and Hughes [12], who increased the pitch angle by offsetting the pivot point toward the trailing edge of the slider. A similar observation has also been reported by Nishihira et al. [13] in an investigation of the dynamic flying behavior of shaped-rail sliders. In the latter study, which came to our attention after completion of this paper, results were obtained which indicated that increased pitch is equivalent to improved bearing stability. Thus, the results of the present investigation appear to be in excellent qualitative agreement with the findings of other researchers, and we are justified in suggesting that the simulation of contacts during start/stop as done in this paper may become an important design step in the evaluation of improved future bearing designs.

One additional point which is of interest in the experimental verification of our contact model is related to acoustic emission data obtained from the head/disk interface [14]. Here, it was observed that acoustic emission is a strong function of bearing design parameters, decreasing to a low value at a critical velocity corresponding to the sliding-to-flying transition velocity. Furthermore, it was found that acoustic emission is a function of surface roughness and slider design, and that frequencies in the acoustic emission spectrum can be observed up to 500 kHz. All of the above trends have been simulated numerically using our contact simulator and are found to be in qualitative agreement with our numerical calculations. Thus, acoustic emission data appear to provide a qualitative verification of our contact simulation model.

Summary

A dynamic simulator has been implemented to study slider/disk collisions in a magnetic recording disk file. Compared to earlier models [4, 5, 7–10], the present simulation has the improvement of an on-line solution to the time-dependent Reynolds equation coupled with the slider dynamics. The simulator represents a substantial improvement over the previous table lookup procedure, since no assumptions had to be made in the new simulator about the air-bearing damping and stiffness parameters. Furthermore, the new simulator is not restricted to small deviations from the equilibrium state, as was the case with the table lookup procedure. Thus, the new scheme can be applied without restrictions to the simulation of arbitrary slider designs.

Future modeling efforts should be directed toward improvements in the representation of the statistics of rough surfaces, both as it affects air flow and solid-body contact. Further study is also needed on the dynamics of the slider/disk collision to replace or improve upon the coefficient-of-restitution approach.

The results indicate that stable and unstable contact sequences for the slider/disk interface occur, depending on the initial conditions and the value of the coefficients of friction and restitution. For constant initial conditions, increases in the coefficient of friction are seen to increase the region for which unstable contact behavior occurs. In addition, increases in the initial disturbance velocity enlarge the region of instability. The studies suggest that slider designs which permit roll motion while minimizing pitch motion may reduce the possibility of head crashes. Furthermore, slider designs with high pitch angles seem to be preferable to those with smaller pitch angles, since high pitch reduces the chances for undesirable front-corner contacts.

On the basis of the results obtained from the simulator, we believe that contact simulation of slider bearings is an important design tool in the evaluation of new slider designs.

Acknowledgment

The work in this paper was supported in part by National Science Foundation Grant No. MSM-8709588 and University Research Initiative Grant No. N0014-86-K-0758.

References

- D. B. Bogy and F. E. Talke, "Mechanics-Related Problems of Magnetic Recording Technology and Ink-Jet Printing," Appl. Mech. Rev. 39, No. 11, 1665-1677 (November 1986).
- R. C. Tseng and F. E. Talke, "Transition from Boundary Lubrication to Hydrodynamic Lubrication of Slider Bearings," IBM J. Res. Develop. 18, No. 6, 534–540 (November 1974).
- T. Kita, K. Kogure, Y. Mitsuya, and T. Nakanishi, "Wear of the Flying Head of a Magnetic Disk File in Mixed Lubrication," ASLE Special Publication 16, pp. 35-40, October 1984; available from the Society for Tribology and Lubrication Engineers, 838 Busse Highway, Park Ridge, IL 60068.
- Y. Kawakubo, Y. Seo, M. Tokuyama, and K. Tanaka, "Head Contact Pressure and Slow Speed Sliding Test on Coated

- Magnetic Disk," *IEEE Trans. Magnetics* MAG-23, 3438-3440 (September 1987).
- J. W. White and A. Nigam, "A Factored Implicit Scheme for the Numerical Solution of Reynolds Equation at Very Low Spacing," J. Lubr. Technol. 102, No. 1, 80-85 (January 1980).
- K. F. Grove, C. Lee, and D. B. Bogy, "Documentation, Explanation, and Convergence Tests for Static and Dynamic Slider Bearing Simulation Computer Programs," *Technical Report No. 13*, Center for Magnetic Recording Research, University of California at San Diego, La Jolla, CA 92093.
- V. Ponnaganti, T. R. Kane, and J. W. White, "Mechanics of Head-Disk Contact/Impact in Magnetic Recording," *IEEE Trans. Magnetics* MAG-23, 3435-3437 (September 1987).
- V. Ponnaganti, T. R. Kane, and J. W. White, "Simulation of Head-Disk Collisions in Magnetic Recording," STLE Preprint No. 87 TC-1C-1; available from the Society for Tribology and Lubrication Engineers, 838 Busse Highway, Park Ridge, IL 60068
- R. C. Benson and F. E. Talke, "The Transition Between Sliding and Flying of a Magnetic Recording Slider," *IEEE Trans. Magnetics* MAG-23, 3441-3443 (September 1987).
- R. C. Benson and F. E. Talke, "The Stability of a Slider Bearing During Transition from Hydrodynamic to Boundary Lubrication," STLE Special Publication 22, pp. 6-11, October 1987; available from the Society for Tribology and Lubrication Engineers, 838 Busse Highway, Park Ridge, IL 60068.
- W. A. Gross, Fluid Film Lubrication, John Wiley & Sons, Inc., New York, 1980.
- H. H. Gatzen and G. F. Hughes, "Flight Attitude and Takeoff/Landing Behavior of a Miniature Winchester Head for Rotary Actuators," STLE Special Publication 22, pp. 133-137, 1987; available from the Society for Tribology and Lubrication Engineers, 838 Busse Highway, Park Ridge, IL 60068.
- H. S. Nishihira, L. K. Dorius, S. A. Bolasna, and G. L. Best, "Performance Characteristics of the IBM 3380 J and K Air Bearing Design," STLE Special Publication 25, pp. 117-123, 1988; available from the Society for Tribology and Lubrication Engineers, 838 Busse Highway, Park Ridge, IL 60068.
- R. C. Benson, R. Sundaram, and F. E. Talke, "A Study of the Acoustic Emission from the Slider/Disk Interface in a 51/4 Inch Hard Disk Drive," STLE Special Publication 25, pp. 87-93, 1988; available from the Society for Tribology and Lubrication Engineers, 838 Busse Highway, Park Ridge, IL 60068.

Received April 13, 1988; accepted for publication September 15, 1988

Richard C. Benson Department of Mechanical Engineering, University of Rochester, Rochester, New York 14627. Dr. Benson received a B.S.E. in mechanical and aerospace science from Princeton University in 1973, an M.S. in mechanical engineering from the University of Virginia in 1974, and a Ph.D. in mechanical engineering from the University of California, Berkeley, in 1977. At Berkeley, he held an IBM Fellowship and studied with Prof. David Bogy. From 1977 to 1980 he worked for the Xerox Corporation as a technical specialist/project manager. In 1980 Dr. Benson joined the Department of Mechanical Engineering at the University of Rochester, where he is currently an associate professor. In 1984 he received the Henry Hess Award, given by the American Society of Mechanical Engineers to honor a publication by a young author. His principal research interest is the mechanics of very flexible structures, particularly with application to the sheets, tapes, and disks found in modern office machinery. In 1986-87 Dr. Benson spent a sabbatical year at the Center for Magnetic Recording Research at the University of California, San Diego. There he collaborated with Prof. Frank Talke in modeling the dynamics of head/disk collisions in "hard" disk magnetic recording. The present paper is one product of that collaboration.

Chisin Chiang Department of Mechanical Engineering, Stanford University, Stanford, California 94305. Mr. Chiang graduated with a B.Sc. degree from the Department of Applied Mechanics and Engineering Sciences at the University of California, San Diego, in 1988. During 1987 and 1988 he worked as an engineering aide in Prof. Talke's laboratories at the Center for Magnetic Recording Research. Mr. Chiang is currently a first-year graduate student in mechanical engineering at Stanford University.

Frank E. Talke Center for Magnetic Recording Research, University of California at San Diego, La Jolla, California 92093. Dr. Talke is a professor of Applied Mechanics and Engineering Sciences at the University of California, San Diego, and holds an endowed chair in the Center for Magnetic Recording Research. He received a Dipl.-Ing degree from the University of Stuttgart, Germany, in 1965, and an M.Sc. and a Ph.D. degree in mechanical engineering from the University of California, Berkeley, in 1966 and 1968, respectively. After graduation from Berkeley, Dr. Talke joined IBM Research in San Jose, California, in 1969, working on various aspects of magnetic recording and ink-jet printing technology. He spent 1984 on sabbatical at UC Berkeley as a visiting professor, and assumed his current position at UC San Diego in March of 1986.